Available online at www.sciencedirect.com
SCIENCE DIRECT®
Applied Thermal Engineering 25 (2005) 1724–1739
APPLIED THERMAL ENGINEERING
www.elsevier.com/locate/apthermeng

Temperature and thermal deformation analysis on scrolls of scroll compressor

Chiachin Lin [a], Yuchoung Chang [b], Kunyi Liang [b], Chinghua Hung [a,*]

[a] *Department of Mechanical Engineering, National Chiao Tung University, 1001 Ta Hsueh Rd., Hsinchu 300, Taiwan*
[b] *Energy and Resources Laboratories, Industrial Technology Research Institute, Chutung, Hsinchu 310, Taiwan*

Received 20 May 2004; accepted 16 November 2004
Available online 28 December 2004

Abstract

The thermal deformation of scrolls significantly affects the hermetic property between scrolls, and thus affects the efficiency of the scroll compressor. An accurate temperature distribution on scrolls must be obtained before the thermal deformation of scrolls can be analyzed. The temperature inside real scrolls in the steady state was experimentally measured. Then, reasonable thermal boundary conditions were applied to perform a heat transfer analysis to determine the temperature distribution on scrolls. Then, the distribution of the thermal deformation on scrolls was analyzed. Finally, fixed and orbiting scrolls were engaged with each other and analyses were performed to determine the stress and deformation distributions at the orbital angle that the maximum compression ratio happens.

Keywords: Scroll; Temperature; Thermal deformation; Finite element analysis

1. Introduction

In related scroll pump research, some researchers have assumed boundary conditions of heat transfer analysis, based on theory, while some measure the temperatures of refrigerant inside

* Corresponding author. Tel.: +886 3 5712121x55160; fax: +886 3 5720634.
E-mail address: chhung@mail.nctu.edu.tw (C. Hung).

1359-4311/$ - see front matter
doi:10.1016/j.applthermaleng.2004.11.008

suction inlet and discharge outlet and the temperature of frame to assume boundary conditions for heat transfer analysis. The rotating speed of orbiting scroll is around 3500 rpm, and the states of chambers change all the time during the compression process. However, conjectures based on theories can only yield the temperature of refrigerant at a certain orbital angle. Therefore, temperature distributions derived by heat transfer analysis with boundary conditions set by these approaches are not generally accepted.

Although the measured temperature of scrolls varies with time, it should do so only within a small range. Therefore, this investigation measures more temperature points inside scrolls without destroying the chambers and the surfaces of scrolls wraps. Reasonable boundary conditions are assumed, depending on the measured temperature data so that the heat transfer analysis yields the most accurate temperature distribution. Then, thermal deformation analysis is performed according to the temperature distribution to help in designing scroll compressors.

2. Temperature-measuring experiment

2.1. Positions of the measuring points

In measuring the temperature of fixed scroll, the scroll wrap may crack if a hole is drilled into the inside of the scroll wrap. The temperature-measuring experiment is thus divided into two stages to ensure that at last the temperature can be measured at the measuring points inside the base of fixed scroll. In the first stage of the experiment, there are 15 measuring points as illustrated in Figs. 1 and 2. In the second stage of the experiment, there are 11 measuring points as illustrated in Figs. 3 and 4. Among which, the points AB, BB, CC1 and CC2 are selected because of that the temperature along the trajectory of the outmost circle of scroll wrap increased from the outside circle to the inner circle, however, it falls along the trajectory of the second circle [1].

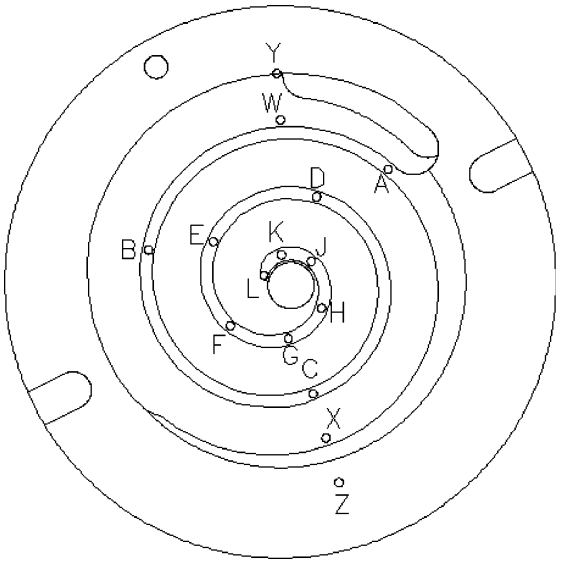

Fig. 1. Positions of the measuring points in the first stage of the temperature-measuring experiment (bottom view).

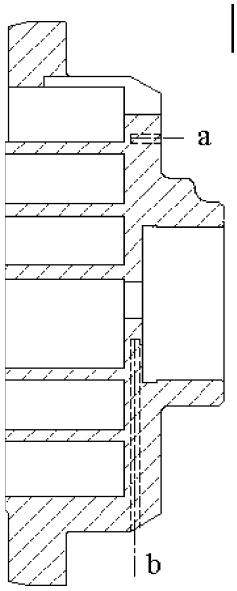

Fig. 2. "a" illustrates the depths at points A, B, C, D, W, X, Y and Z, and "b" illustrates the depths at points E, F, G, H, J, K and L in the first stage of the temperature-measuring experiment. (Positions are not accurately depicted.)

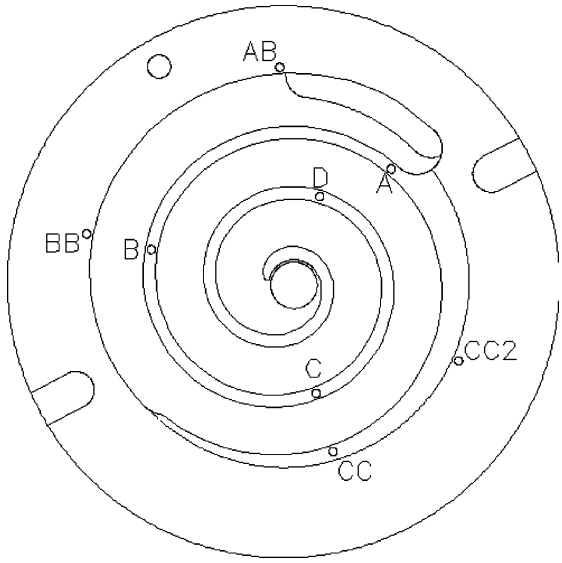

Fig. 3. Positions of the measuring points in the second stage of the temperature-measuring experiment. (Bottom view.)
Note: Positions of point E, H and L are the same in both stages of the temperature-measuring experiment.

Additionally, one thermocouple is placed at each of the suction inlet and discharge outlet to measure the temperature of refrigerant in the first stage of the experiment, and one thermocouple is placed at discharge outlet in the second stage of the experiment. Furthermore, the points E, H and L are located at the same place in both the first and second stage of the experiment.

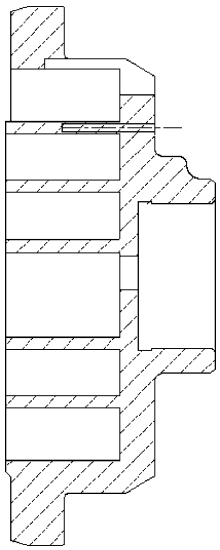

Fig. 4. Sketch of the depths at points A, B, C and D in the second stage of the temperature-measuring experiment. (Positions are not accurately depicted.) *Note*: Depths of points E, H, L, AB, BB, CC1 and CC2 are the same as those of the points in the first stage of the temperature-measuring experiment.

The temperature of orbiting scroll is not measurable since thermocouple cannot be installed. The temperature closest to the orbiting scroll that is measurable is the temperature near the oil chamber in frame. Accordingly, three points in the frame are selected both in the first stage and the second stage of the experiment. These are points FA, FB and FC in Fig. 5.

2.2. The results of the temperature-measuring experiment

Table 1 presents the temperature of refrigerant in suction inlet and discharge outlet in the first stage of the experiment, and other experimental results. Table 2 presents the temperature of refrigerant in suction inlet and discharge outlet in the second stage of the experiment, and other

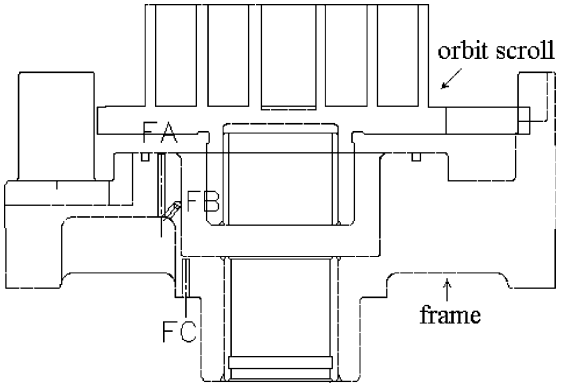

Fig. 5. Measuring points in the frame.

Table 1
Temperatures at nodes measured in the first stage of the experiment

	First time	Second time
Suction pressure	5.34 kg/cm^2	5.34 kg/cm^2
Discharge pressure	20.85 kg/cm^2	20.85 kg/cm^2
Point A in fixed scroll base	63.0 °C	63.1 °C
Point B in fixed scroll base	68.2 °C	68.3 °C
Point C in fixed scroll base	75.2 °C	75.3 °C
Point D in fixed scroll base	77.1 °C	77.2 °C
Point E in fixed scroll base	79.1 °C	79.2 °C
Point F in fixed scroll base	82.3 °C	82.4 °C
Point G in fixed scroll base	86.0 °C	86.0 °C
Point H in fixed scroll base	89.3 °C	89.3 °C
Point J in fixed scroll base	93.6 °C	93.5 °C
Point K in fixed scroll base	93.9 °C	94.0 °C
Point L in fixed scroll base	97.4 °C	97.4 °C
Point W in fixed scroll base	61.2 °C	61.3 °C
Point X in fixed scroll base	68.8 °C	68.6 °C
Point Y in fixed scroll base	58.7 °C	58.8 °C
Point Z in fixed scroll base	65.7 °C	65.8 °C
Point FA in frame	64.6 °C	64.7 °C
Point FB in frame	64.0 °C	64.0 °C
Point FC in frame	64.3 °C	64.4 °C
Refrigerant inside discharge outlet	107.0 °C	106.9 °C
Refrigerant inside suction inlet	47.1 °C	47.1 °C

Table 2
Temperatures at nodes measured in the second stage of the experiment

	First time	Second time
Suction pressure	5.34 kg/cm^2	5.34 kg/cm^2
Discharge pressure	20.85 kg/cm^2	20.85 kg/cm^2
Point A in fixed scroll wrap	58.1 °C	57.2 °C
Point B in fixed scroll wrap	63.6 °C	62.8 °C
Point C in fixed scroll wrap	70.4 °C	69.6 °C
Point D in fixed scroll wrap	78.9 °C	77.9 °C
Point E in fixed scroll base	80.2 °C	79.0 °C
Point H in fixed scroll base	90.5 °C	89.6 °C
Point L in fixed scroll base	97.6 °C	96.5 °C
Point AB in fixed scroll base	52.5 °C	52.0 °C
Point BB in fixed scroll base	61.3 °C	60.5 °C
Point CC1 in fixed scroll base	66.7 °C	65.7 °C
Point CC2 in fixed scroll base	66.1 °C	65.1 °C
Point FA in frame	65.0 °C	64.0 °C
Point FB in frame	64.5 °C	63.5 °C
Point FC in frame	65.1 °C	64.3 °C
Refrigerant inside discharge outlet	106.7 °C	105.7 °C

experiment results. Additionally, in the first and second stage of the experiment, most temperature data recorded around 10 min vary by no more than 1 °C, and the largest variation in temperature is only 2.3 °C, demonstrating that the temperature distribution of scrolls varies within a small range in the steady state, as assumed at beginning of this investigation.

Comparing the temperatures of points E, H, L, FA, FB and FC and the temperature of discharge outlet both in Tables 1 and 2. Finding that the differences of the temperatures are very small. Therefore, the states of the compressor in the two stages of the experiment seem to be the same.

Therefore, all of the temperatures measured in the first stage of the experiment and the temperatures at points A, B, C and D in the scroll wrap and points AB, BB, CC1 and CC2 in the base of the fixed scroll in the second stage of the experiment, are considered in a finite element analysis to yield the temperature distribution, the thermal deformation and the stress distribution of the scrolls.

3. Finite element analysis

3.1. Software introduction

The software packages used in this analysis are I-DEAS and ABAQUS. I-DEAS is a pre-processor to be used to construct the meshed model, and ABAQUS is a software package of finite element analysis.

A model similar in shape to the real scrolls is conducted and meshed by using I-DEAS. After an ABAQUS input file was generated by I-DEAS, including data related to the meshed model, the material properties, the boundary conditions and the constrains, ABAQUS was used to perform the simulation.

Table 3
Dimensions of scrolls

The parameter of designing scrolls	Parameter value
The geometry shape of scrolls	Standard expansion involute
The thickness of scroll wrap	2.6 mm
The height of scroll wrap	25 mm
The radius of base circle	2.06 mm
The radius of mill	5.15 mm
The extended value of scrolls	0.0 mm
The pitch of scrolls	12.96 mm
The thickness of fixed scroll base plank	8 mm
The outer radius of fixed scroll base plank	96 mm
The thickness of orbit scroll base plank	7 mm
The outer radius of orbit scroll base plank	92 mm
Orbit radius	3.83 mm
Orbit angle	−21°

Note: The effective numbers shown here were decreased to protect the intellectual property rights.

Table 4
Material properties [2–4]

Type of the material of scrolls	Grey cast iron FC250
Elasticity modulus	113 GPa
Poisson ratio	0.26
Density	7.15E−6 kg/mm^3
Coefficient of expansion	13.3E−6/°C
Coefficient of heat transfer	0.0526 W/mm°C
Specific heat	500.0 J/kg°C
Tensile strength	260 MPa
Fatigue strength	128 MPa

3.2. Dimensions of scrolls

Table 3 lists the dimensions of scrolls. Maximum compression ratio happens while the orbital angle is −21°, and maximum stress happens with the maximum compression ratio. Therefore determining the required data that pertain to the design as the orbital angle is −21°.

3.3. Material properties

The material properties used in finite element analysis are the same as those of real fixed scroll and the orbiting scroll. The real scrolls are made from gray cast iron FC250, whose material properties are illustrated in Table 4.

4. Heat transfer analysis

4.1. Boundary conditions of heat transfer analysis

Since the temperature varies within a very small range at any given point as the compressor is in a steady state, the temperatures in the regions near to the measuring points in the scrolls are assumed to be the corresponsive measured temperatures. The temperature boundary conditions are as follows.

- *Boundary conditions on fixed scroll:* (Please refer to Fig. 1 for the positions of the measuring points.)
  1. The temperatures at the nodes on the outermost layer of the bottom of the fixed scroll are the same as those of the refrigerant in the suction inlet.
  2. At points A–D, the temperatures at the nodes vertically from the tip of the scroll wrap to the root of the scroll wrap are the same as the corresponsive measured temperature; the temperatures at the nodes vertically from the middle of the base to the chamber are the same as the corresponsive measured temperature.
  3. At points E–L, the temperatures at the nodes vertically from the tip of the scroll wrap to the middle of the base are the same as the corresponsive measured temperature.

4. At points W, X, Y, Z, AB, BB, CC1 and CC2, the temperatures of the nodes vertically from the middle of the base to the chamber are the same as the corresponsive measured temperature.

The shape and positions of the chambers in scrolls are symmetrical, so the temperature distributions of a couple of symmetric chambers should be very similar when the compressor is in a steady state. Accordingly, the temperatures in symmetrical positions in the orbiting scroll and the fixed scroll should be very similar. Consequently, the temperatures, at couples of symmetric positions separately in the fixed and the orbiting scroll wraps, are assumed to be equal. Besides,

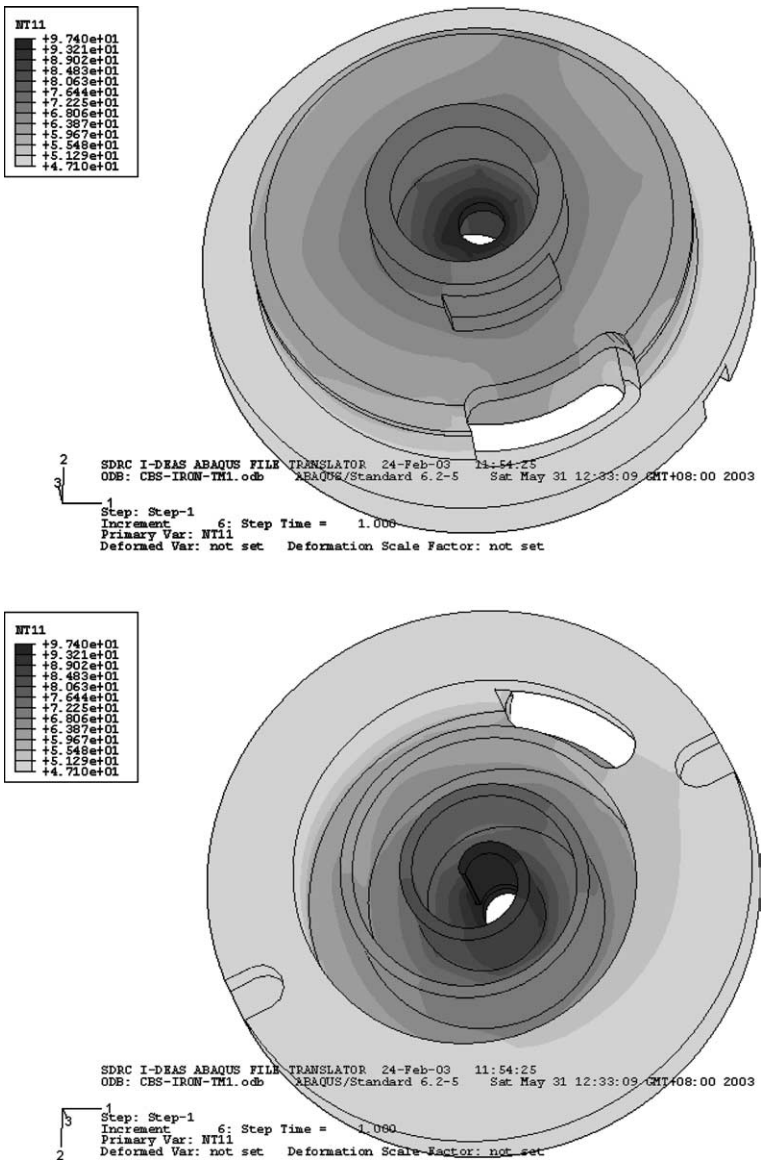

Fig. 6. Temperature distribution in the fixed scroll.

the bottom surface of the orbiting scroll base and the bearing are also assumed to be the same temperature as that at the nearest measurable positions in the frame.

- *Boundary conditions for orbiting scroll:*
  1. The temperature at the nodes on the outermost layer in the bottom of the orbiting scroll is the same as that of the refrigerant in the suction inlet.
  2. At the symmetrical positions on orbiting scroll, corresponding to points A–L on fixed scroll, the temperatures of the nodes vertically from the tip of the scroll wrap to the root of the scroll wrap equal those at corresponsive points A–L.

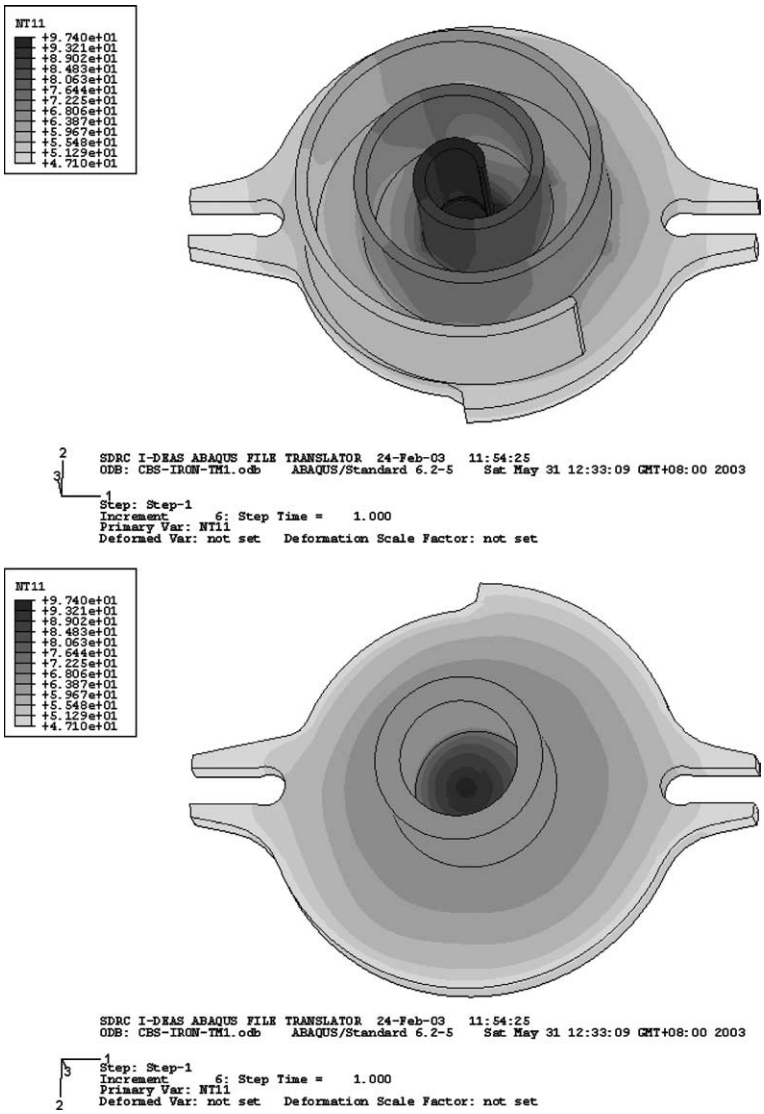

Fig. 7. Temperature distribution in the orbiting scroll.

3. The temperature of the nodes on the base near the bearing of the orbiting scroll are the same as that at point FA in the frame; the temperature of the nodes on the outermost layer of bearing of orbiting scroll are the same as that at point FB; the temperatures at the nodes on the bottom of the bearing of the orbiting scroll are the same as that at point FC. (Please refer to Fig. 5 for the position of the measuring points.)

Furthermore, the temperature distribution in the scrolls varies within a small range while the compressor is in a steady state. Consequently, the following boundary conditions are assumed in the heat transfer analysis.

1. No heat is transferred between the fixed and the orbit scroll.
2. No heat is transferred between the scrolls and the external environment, so the scrolls are adiabatic.

4.2. Results of heat transfer analysis

Figs. 6 and 7 plot the obtained temperature distribution. The figures reveal that the temperature uniformly falls from the center of the scrolls to the outer circle.

5. Thermal deformation analysis

5.1. Constraints on thermal deformation analysis

The results of the temperature distribution analysis are considered in the thermal deformation analysis. Some constrains are applied to the thermal deformation analysis according to the situation of real scrolls.

- *Initial temperature:* 25.0 °C.
- *Constraints on fixed scroll:*
  1. The freedom in the Z direction in the surface of the fixed scroll base is constrained.
  2. The regions of contact between the fixed scroll and the frame include clearance. Accordingly, the displacement in the radial direction is assumed to equal the real clearance. (Please refer to Fig. 8 for the contact regions.)
  3. The freedom in the normal direction of the lateral wall of the key groove of the fixed scroll is constrained to prevent rotation of the fixed scroll.

- *Constraints on the orbiting scrolls: Note*: The X axis is in the direction of axis 1; the Y axis is in the direction of axis 2, and the direction Z axis is in the direction of axis 3. See Fig. 7, for example.
  1. The freedom in the Z direction in the surface that contacts the frame thrust plane is constrained.
  2. In the lateral wall of the key groove of the orbiting scroll, contact the key of the Oldham ring; the freedom is constrained in the normal direction to prevent self-rotation of the orbiting scroll.

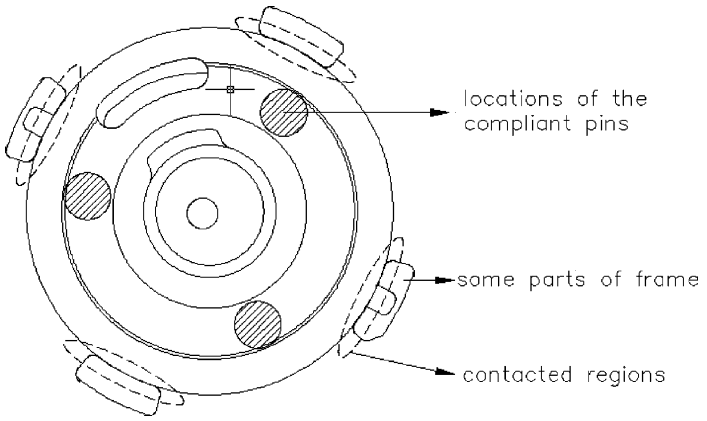

Fig. 8. The elliptic areas drawn by dashed line indicate where the fixed scroll contact the frame. And the circular areas with oblique lines are where the back pressure is exerted (top view).

3. The freedom in the X and Y directions in the inner wall of the orbiting scroll bearing is constrained.
4. The freedom in the Z direction in the top of the orbiting scroll bearing is constrained.

5.2. Results of thermal deformation analysis

In both the fixed scroll and the orbiting scroll, the greatest deformation affected by temperature is the scroll wraps near the discharge outlet. The maximum deformation value in the fixed scroll is 28.60 μm. The maximum deformation value in the orbiting scroll is 29.38 μm. Both extreme values were obtained before engaging both fixed and orbiting scrolls.

6. Stress and deformation analyses after scrolls engage with each other

6.1. Constraints applied analysis after the scrolls engage with each other

The following constraints are applied in the stress and deformation analyses after the scrolls engage with each other:

- *Initial temperature:* 25.0 °C.
- *Constraints on fixed scroll:* The constraints are the same as the second and third constraints on fixed scroll in the thermal deformation analysis.
- *Constraints on the orbiting scroll:* All of the constraints are the same as those on the orbiting scroll in the thermal deformation analysis.
- *Pressure conditions:*
  1. The three used thin circle planks all have the same sectional area as compliant pins to give back-pressure to the fixed scroll at the location of the compliant pins on the surface of the base of the fixed scroll. (The locations of compliant pins are marked in Fig. 8.)

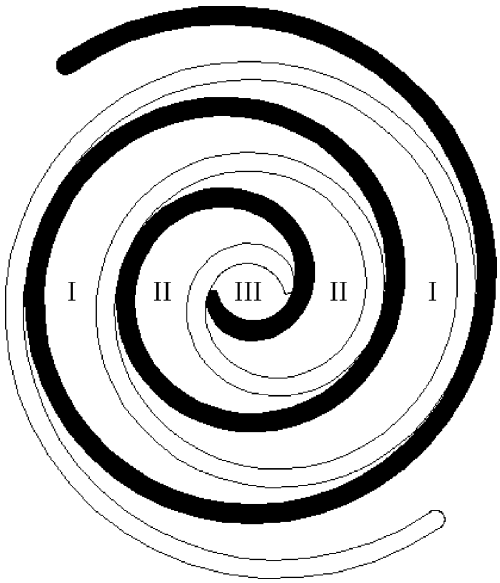

Fig. 9. Chambers I, II and III shaped as the orbit angle is −21°.

2. Fig. 9 presents three order of chambers as the orbital angle is −21°, they are chambers I, II and III. Accordingly, the pressure in the lateral wall of the scroll wrap, which surrounds each chamber, is assumed to be equal to that in the surrounded chamber.
3. In Fig. 9, the pressure in the lateral wall of the scroll wrap, which does not surround the chambers, is assumed to equal the pressure in the low-pressure room.

Table 5 presents the back-pressure and the pressure in each order of chamber. These values are calculated from Polytropic Theoretical Formula [1].

6.2. Results of stress analysis and discussions

Fig. 10 presents where the stress concentrated. In the fixed scroll, the stresses at all nodes are below 125 MPa and below the fatigue stress. Consequently, safety is not a concern. In the orbiting scroll, the region with greatest stress value is in the rim of the top inside bearing, and the stress is in the range of 149.7–160.5 MPa. Although these values exceed the fatigue stress, the mean stress

Table 5
Back pressure and pressure of each order chamber

Back pressure	7.30 MPa
The pressure of refrigerant in low pressure Room	0.63 MPa
The pressure of chamber I	0.86 MPa
The pressure of chamber II	2.25 MPa
The pressure of chamber III	2.17 MPa
The pressure of refrigerant in high pressure room	2.16 MPa

Note: The effective numbers shown here were decreased to protect the intellectual property rights.

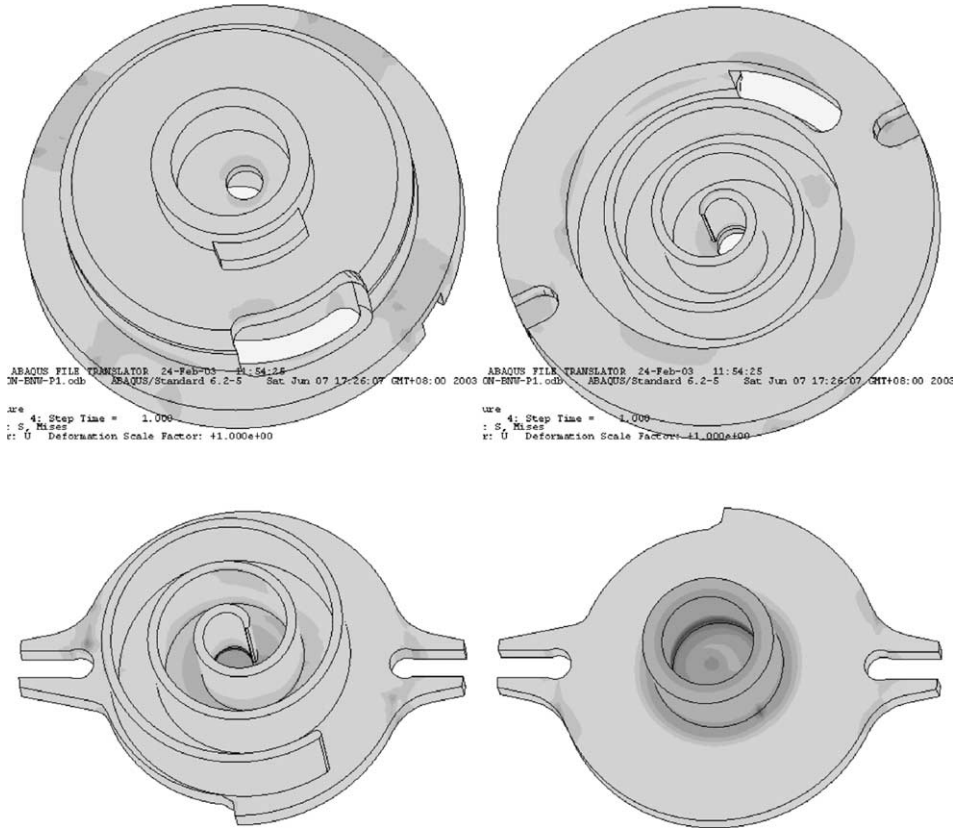

Fig. 10. The darker gray areas are the regions where stresses concentrated.

of FC250 is zero; therefore the fatigue stress of FC250 is 128 MPa means that the alternating stress is 128 MPa. Moreover, the stresses in the region of maximum stress in the orbiting scroll are never below 0 MPa. If the minimum stress is assumed to be 0 MPa, then the alternating stress is approximately 80.25 MPa, which is smaller than 128 Mpa. Therefore, safety is not an issue.

6.3. Results of deformation analysis and discussions

Fig. 11 presents that the region of smallest deformation in the fixed scroll are mainly in the bottom and lateral wall of fixed scroll base. Some others are the tip in some parts of the scroll wrap, and the deformation is around 3 μm. The region of greatest deformation in the negative Z direction is located in the two regions of the contact between the fixed scroll and the frame, perhaps because the fixed scroll base does not contact the orbiting scroll base in the regions; therefore the obstruction is smaller than other regions. The region of greatest deformation in the Z direction is located in the top of the cylinder of fixed scroll. But the region of second greatest deformation, in the vicinity of discharge outlet of fixed scroll wrap, is more important than the region of greatest deformation. The maximum deformation value in the region of second greatest deformation in the Z direction of the fixed scroll is 24.50 μm.

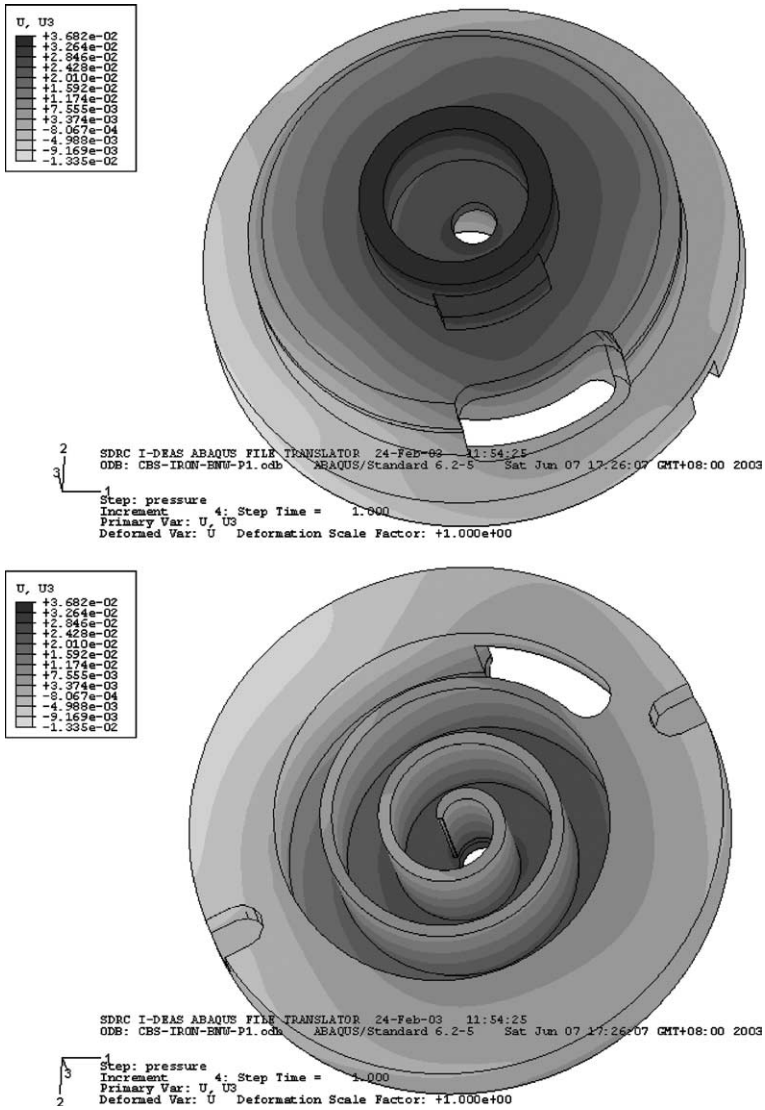

Fig. 11. Deformation distribution in fixed scroll.

Fig. 12 reveals that the deformation distribution in the orbiting scroll is more regular than the fixed scroll. The greatest deformation in the Z direction is centered on the part of the scroll wrap near chamber III, as presented in the figure. The greatest deformation in the direction of negative Z is centered on the bearing. The deformation in Z direction is more important than that in negative Z direction. The maximum deformation in Z direction of the orbiting scroll is 29.31 μm.

The deformation results of fixed and orbiting scrolls can be used as reference for the future design, for instance, the aluminum scrolls. Above all, the greatest deformation of scrolls in Z direction should be given more concerns for engineers.

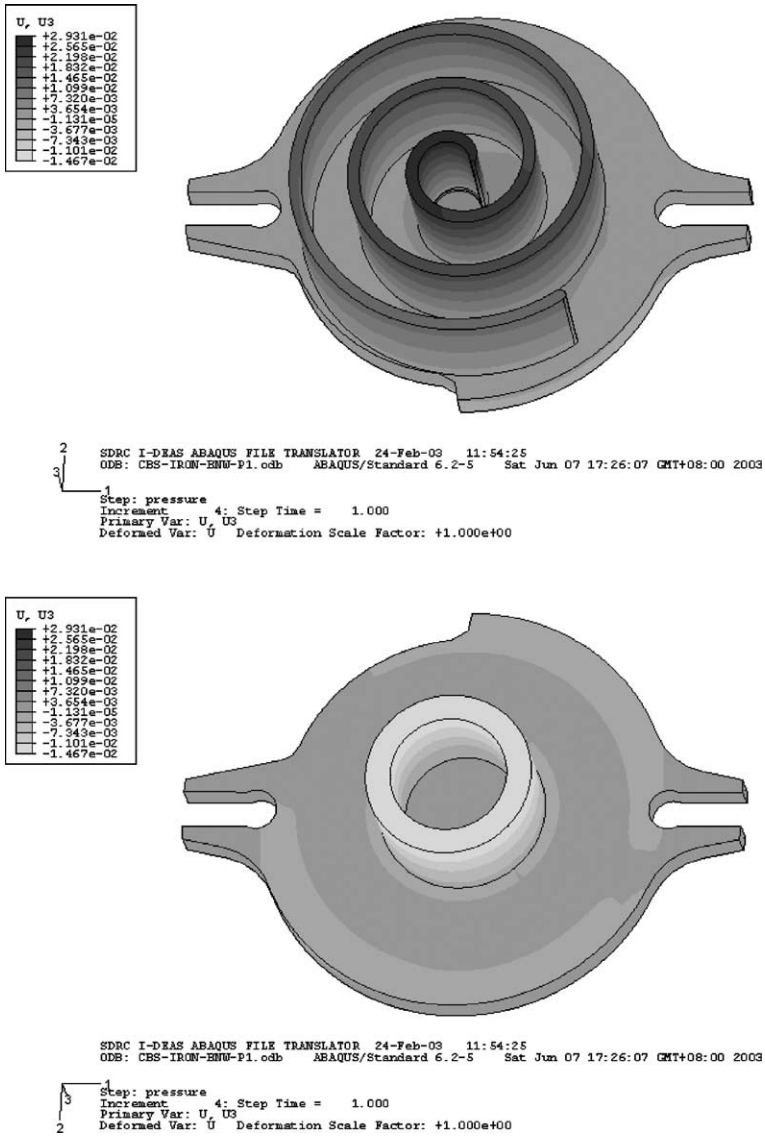

Fig. 12. Deformation distribution in orbiting scroll.

7. Conclusions

This investigation first provides a method to measure the temperature of real scrolls, refrigerant, and frame. The method is based on the premises that the chamber and the surface of the scroll wrap must not be destroyed. Then, combining the temperature data and FEM to yield the temperature, stress and deformation distributions of the scrolls, which are close to the real situation. These procedures can be extended to other scroll compressors with different dimensions. In this

investigation, the results are worth referring to design similar scroll compressors with cooling capacity about 6600 kcal/h. The following conclusions are drawn.

1. The variation of temperature distribution in scrolls in a steady state is small. Accordingly, an analysis can be feasibly based on the temperature data.
2. The heat transfer analysis yields the result that the temperature declines from the center of scrolls to the outer circle.
3. The thermal deformation analysis without considering the effect of pressure yields the maximum deformation of the fixed scroll is 28.60 μm, and that of the orbiting scroll is 29.38 μm.
4. The stress analysis after the scrolls engage with each other yields the stress concentration regions in the fixed scroll are the region of contact between the fixed scroll and the frame, the key grooves and the area around the discharge outlet. The stress concentration regions in the orbiting scroll are the key grooves, the vicinity of the chamber III in the orbiting scroll base, the root of the orbiting scroll wrap, the inside of the bearing and the vicinity of the join region between the orbiting scroll base and the bearing.
5. After comparing the stress values, yielded by the stress analysis after the scrolls engage with each other, with the fatigue stress, safety is thus not an issue for the current design.
6. The deformation analysis after the scrolls engage with each other yields the deformation distribution of the scrolls. The maximum deformation value of the fixed scroll is 24.50 μm. The maximum deformation value of the orbiting scroll is 29.41 μm.

Acknowledgement

The authors greatly appreciate the help of the Rechi Precision Corporation, Taiwan, for the temperature-measuring experiment.

References

[1] S. Sunder, J.L. Smith, Jr., Kissing heat transfer between the wraps of a scroll pump, in: Proceedings of the 1996 ASME International Mechanical Engineering Congress and Exposition, vol. 36, Atlanta, GA, USA, November 1996, pp. 133–149.
[2] J. Yamabe, M. Takagi, T. Matsui, T. Kimura, M. Sasaki, Development of disc brake rotors for trucks with high thermal fatigue strength, JSAE Review 23 (1) (2002) 105–112.
[3] http://supplier.saab.com/std/docs/510125.pdf.
[4] http://www.matweb.com/search/SpecificMaterial.asp?bassnum=MCFE14.